VOLUME 113, NUMBER 9
APRIL 24, 1991

JOURNAL
OF THE
AMERICAN
CHEMICAL
SOCIETY

Molecular Orbital Analysis of the Orientation-Dependent Barrier to Direct Exchange Reactions

Davide M. Proserpio,[†] Roald Hoffmann,*[,†] and R. D. Levine*[,‡]

Contribution from the Department of Chemistry and Materials Science Center, Cornell University, Ithaca, New York 14853-1301, The Fritz Haber Research Center for Molecular Dynamics, The Hebrew University, Jerusalem 91904, Israel, and the Department of Chemistry and Biochemistry, University of California, Los Angeles, California 90024-1569.
Received June 11, 1990

Abstract: After a general introduction to the current state of potential energy functions for delineating the steric requirements of exchange reactions, we proceed to a qualitative, Walsh-diagram-based orbital analysis of the preferred geometry approach to the barrier to such reactions. Extended Hückel calculations, perturbation theory, and a frontier orbital perspective are used to analyze the X + H_2 (collinear, due to the controlling role of the singly occupied highest molecular orbital), X + HX, X + HY (also collinear), H + X_2 (bent, due to interaction with a relatively low lying unfilled orbital), H + XY (a preference for direction of attack depending on relative electronegativities), M + X_2, M + XY, M + HX (collinear approach slightly preferred), X + XY, and triplet O atom reactions.

Introduction

Concerted atom exchange reactions, even when exothermic, do typically have an activation barrier. The rate of such reactions is often lower that the collision rate computed for hard spheres with enough energy to surmount this barrier.[1] The venerable collision theory of chemical kinetics introduces therefore an ad hoc "steric factor" as the ratio of the observed to computed rates. The origin of the correction was clearly understood: the reaction has not only energetic but also steric requirements. However, no prescription for computing this factor was provided.

An early success of transition-state theory[1] was that it produced a quantitative account of the steric factor. In terms of the thermodynamic formulation of the theory, the steric factor is due to the entropy loss in going from the free rotation in the reagents to the very restricted rotation in the transition state.

Transition-state theory by its very nature deals with thermal reactants. The direct experimental demonstration of the steric requirements of exchange reactions[2,3] requires the collision of oriented reactants. Indeed, in the entire area of molecular reaction dynamics,[4] progress has been due to the use of selected reagents which are necessarily not in equilibrium.

Exact dynamical computations (whether classical or quantum) can, of course, begin with a sharply defined initial state and hence are directly relevant to scattering experiments. Moreover, with proper averaging over the initial conditions they determine the magnitude of the steric factor. Such computations require as input the potential energy function (which varies with the interatomic distances) of the systems.[5,6]

In principle, the potential energy function can be determined by the standard methods of ab initio quantum chemistry.[7-10] In

[†] Cornell University.
[‡] The Hebrew University.

(1) Laidler, K. J. *Chemical Kinetics*; Harper and Row: New York, 1987.
(2) Brooks, P. R. *Science* **1976**, *193*, 11. Stolte, S. *Ber. Bunsenges. Phys. Chem.* **1982**, *86*, 413. Bernstein, R. B.; Herschbach, D. R.; Levine, R. D. *J. Phys. Chem.* **1987**, *91*, 5365.
(3) Bernstein, R. B. *Chemical Dynamics via Molecular Beam and Laser Techniques*; Oxford University Press: New York, 1982.
(4) Levine, R. D.; Bernstein, R. B. *Molecular Reaction Dynamics and Chemical Reactivity*; Oxford University Press: New York, 1987.
(5) Hirst, D. M. *Potential Energy Surfaces*; Taylor and Francis: London, 1985. Truhlar, D. G., Ed. *Potential Energy Surfaces and Dynamics Calculations*; Plenum: New York, 1981.
(6) Schatz, G. C. *Rev. Mod. Phys.* **1989**, *61*, 669.
(7) Truhlar, D. G.; Steckler, R.; Gordon, M. S. *Chem. Rev.* **1987**, *87*, 217.
(8) Mezey, P. G. *Potential Energy Hypersurfaces*; Elsevier: Amsterdam, 1987.

0002-7863/91/1513-3217$02.50/0

practice this has only been implemented, for a sufficiently wide range of interatomic distances, for a rather limited set of reactions.

Potential energy functions for use as input for (exact or approximate) dynamical computations are currently being generated primarily by a valence bond semiempirical approach. The most common procedure, knows as LEPS,[5] is based on the zeroth order, London-type approach which is strictly valid only for S-state atoms. An LEPS-type function will usually predict a collinear transition state. More recently, a refined, diatomic-in molecules (known as DIM) procedure has been extensively applied.[11-14] A large data set is required as input for the semiempirical DIM procedure which does, however, lead to results often qualitatively different from that of the simple LEPS limit. In particular we note that it often favors a not strictly collinear approach.

For stable ABC molecules, Walsh[15] considered the variation of the molecular orbital energies with bend angle. In this fashion he was able to correlate the equilibrium geometry of the molecule with the number of valence electrons. The Walsh procedure can equally well be used to examine the bend angle for which the ABC transition state in the A + BC reaction has the lowest energy. A qualitative molecular orbital interpretation of the steric requirements of atom exchange reactions was thereby provided.[16-18]

In this paper we take the molecular orbital approach one step further by using computed, rather than estimated, molecular orbital energies. The computations are performed within the extended Hückel formalism.[19] This is a very approximate MO approach with real limitations for geometrical optimization. It does, however, seem to get the bending of the molecule right. Moreover, it has the advantage of transparency in that it provides a very direct, perturbation theory based on connection to simple orbital concepts. In this way it retains the advantage of qualitative methods of correlating the geometry of the transition state to orbital occupancy in the reagents.

Strictly speaking we need to compute the entire potential energy function. In this preliminary attempt we pursue a more modest goal, justified by the following consideration: To a zeroth approximation one can continue to adopt for the dynamics the old collision theory point of view with one essential change.[4,20-22] To account for the steric requirements it is necessary to regard the barrier to reaction as depending on the orientation of the reactants (that is, on the ABC bend angle for the A + BC reaction). The object of our computation is to determine this dependence.

The concept of an orientation-dependent barrier to reaction is an important one because it allows "inversion" from experimental data. In other words, dynamical stereochemistry[23] experiments can provide a rather direct handle for a key feature of the potential energy function. Such an inversion has indeed been demonstrated.[24,25]

Already at the level of the orientation-dependent barrier to reaction there can be a meeting of theory and experiment. Other aspects of dynamical stereochemistry can be found in two recent conference proceedings[23,26] and, in general, in the reports of any recent conference dealing with the dynamics of molecular collisions (e.g. refs 27-29). The available experimental and computational results show that such exchange reactions which proceed without an activation barrier (e.g. certain ion–molecule reactions[4,30,31]) have their steric requirements dominated by the anisotropy of the long-range physical forces. Here, however, we are concerned with activated atom exchange for which the orientation dependence of the chemical barrier is the relevant factor.

We note here a distinction between two basic ways in which orientation effects can be manifested in the A + BC reaction. The first, the one of concern here, is the orientation dependence of the barrier to reaction which governs the reactivity. The second regards the dynamics of the trajectories of real molecules as they traverse the potential energy surface in their approach motion to the barrier. The anisotropy of the long-range physical forces and, at the shorter ranges, of the chemical forces en route to the barrier can orient the BC molecule during the approach of A. Time scales of motion are then important as this reorientation is particularly significant for lower velocity collisions and/or if the longer range force is very anisotropic. It is of relevance in understanding the reaction of initially oriented reactants (whether the initial orientation is achieved in the gas phase[32] or via using a condensed medium[33]). It is also of prime importance in understanding the reaction when BC is initially rotationally excited.[34,35] Irrespective, however, of whether BC did or did not significantly reorient during the approach motion to the barrier, reactivity is determined by the orientation dependence of the barrier itself.

When the BC bond is significantly stretched, the orientation dependence of the barrier can change.[36] In extreme cases even new reaction mechanisms can become feasible. An example is the H + H_2 reaction which ordinarily proceeds via collinearly dominated abstraction. At collision energy above 20 kcal mol^{-1} or so, a new insertion-type mechanism, with a sideways approach, becomes feasible.[37] For vibrationally excited (e.g. laser pumped) reagents the cone of acceptance typically opens up.[38] Here we shall not explore such dependence in detail. In practice we have, however, varied the BC bond distance so as to verify that our results do not change in a significant way when the BC bond is somewhat stretched.

Finally we note that the transparency of the extended Hückel procedure and its direct tie to a frontier orbital perspective make it useful in another way. Even if the complete surface is not reliable, identification of the primary interactions (i.e. which orbitals govern a linear or nonlinear geometry) could lead to the optimum functional form for describing a surface. Better calculations could be fitted to the functional form and used in dynamical studies.

The Orientation-Dependent Barrier to Reaction

A simple interpretation of the bonding at the barrier for reaction can be obtained by considering the occupancy of the molecular orbitals for the ABC system.[4,16-18] Following the mode of presentation introduced by Walsh[15] in the study of the geometry of stable ABC molecules, we consider the orbital energies vs the ABC bend angle.

(9) Lawley, K. P., Ed. *Ab initio Methods in Quantum Chemistry*; Wiley: New York, 1987.
(10) Dykstra, C. E. *Ab initio Calculation of the Structures and Properties of Molecules*; Elsevier: Amsterdam, 1988.
(11) Tully, J. C. *Adv. Chem. Phys.* **1980**, *42*, 63.
(12) Kuntz, P. J. *Ber. Bunsenges. Phys. Chem.* **1982**, *86*, 413.
(13) Duggan, J. J.; Grice, R. *J. Chem. Phys.* **1983**, *78*, 3842.
(14) Last, I.; Baer, M. *J. Chem. Phys.* **1984**, *80*, 3246.
(15) Walsh, A. D. *J. Chem. Soc.* **1953**, 2260, 2266, 2288.
(16) Herschbach, D. R. *Adv. Chem. Phys.* **1966**, *10*, 319.
(17) McDonald, J. D.; Le Breton, P. R.; Lee, Y. T.; Herschbach, D. R. *J. Chem. Phys.* **1972**, *56*, 769. Carter, C. F.; Levy, M. R.; Grice, R. *Faraday Discuss. Chem. Soc.* **1973**, *55*, 357.
(18) Mahan, B. H. *Acc. Chem. Res.* **1975**, *8*, 55.
(19) Hoffmann, R.; Lipscomb, W. N. *J. Chem. Phys.* **1962**, *36*, 2179, 3489. Hoffmann, R. *Ibid.* **1963**, *39*, 1397.
(20) Smith, I. W. M. *J. Chem. Educ.* **1982**, *59*, 9.
(21) Jellinek, J.; Pollak, E. *J. Chem. Phys.* **1983**, *78*, 3014.
(22) Levine, R. D.; Bernstein, R. B. *Chem. Phys. Lett.* **1984**, *105*, 467.
(23) Special issue: *J. Phys. Chem.* **1987**, *91*, (21).
(24) Bernstein, R. B. *J. Chem. Phys.* **1985**, *82*, 3656.
(25) Loesch, H. J.; Hoffmeister *J. Chem. Soc., Faraday Trans. 2* **1989**, *85*, 1249.
(26) Special issue: *J. Chem. Soc., Faraday Trans. 2* **1989**, *85*, (8).
(27) Whitehead, J. C., Ed. *Selectivity in Chemical Reactions*; Kluwer: Dordrecht, 1987.
(28) *Faraday Discuss. Chem. Soc.* **1987**, 84.
(29) Vetter, R.; Vigue, J., Eds. *Recent Advances in Molecular Reaction Dynamics*; CNRS: Paris, 1986.
(30) Clary, D. C. *Mol. Phys.* **1984**, *53*, 3.
(31) Levine, R. D.; Bernstein, R. B. *J. Phys. Chem.* **1988**, *92*, 6954.
(32) Bernstein, R. B.; Levine, R. D. *J. Phys. Chem.* **1989**, *93*, 1687. Loesch, H. *J. Chem. Phys.* **1986**, *104*, 213.
(33) Benjamin, I.; Liu, A.; Wilson, K. R.; Levine, R. D. *J. Phys. Chem.* **1990**, *94*, 3937.
(34) Loesch, H. J. *J. Chem. Phys.* **1987**, *112*, 85.
(35) Kornweitz, H.; Persky, A.; Levine, R. D. *Chem. Phys. Lett.* **1986**, *128*, 443.
(36) Schechter, I.; Kosloff, R.; Levine, R. D. *Chem. Phys. Lett.* **1985**, *121*, 297.
(37) Schechter, I.; Levine, R. D. *Int. J. Chem. Kinet.* **1986**, *18*, 1023.
(38) Schechter, I.; Kosloff, R.; Levine, R. D. *J. Phys. Chem.* **1986**, *90*, 1006.

Table I. Atomic Parameters Used in the Calculations

atom	orbital	H_{ii} (eV)	ζ_1	r_{cov} (Å)
F	2s	−40.0	2.425	0.71
	2p	−18.1	2.425	
Cl	3s	−26.3	2.183	0.99
	3p	−14.2	1.733	
Br	4s	−22.07	2.588	1.14
	4p	−13.1	2.131	
I	5s	−18.0	2.679	1.33
	5p	−12.7	2.322	
Li	2s	−5.4	0.650	1.52
	2p	−3.5	0.650	
Na	3s	−5.1	0.733	1.86
	3p	−3.0	0.733	
K	4s	−4.34	0.874	2.27
	4p	−2.73	0.874	
Rb	5s	−4.18	0.997	2.47
	5p	−2.6	0.997	
O	2s	−32.3	2.275	0.60
	2p	−14.8	2.275	
H	1s	−13.6	1.30	0.37

The calculations are performed with the extended Hückel method[19] with weighted H_{ij}'s.[39] In the spirit of choosing a location on the surface characteristic of the onset of chemical forces, a distance is selected at which significant orbital interaction between the approaching atom and the diatomic molecule occurs. This is done in the following way: we calculate the overlap population (OP) between A and BC for different distances (d) in the linear geometry. A separation yielding an OP between 0.09 and 0.11 is chosen, and then it is fixed as angular variations are made. When this value is impossible to reach, we look at the OP for B–C, compared to the value for the isolated molecule (OP_{eq}). We select the distance when the difference (OP_{eq} − OP) is between 0.09 and 0.11. Using these criteria we found in general that $d = [r_1 + r_2 + 0.4\ (1)$ Å], where r_1 and r_2 are the covalent radii of the adjacent atoms. The bond distance of the reactant diatomic is kept at its value for the isolated molecule. We did, however, verify that our conclusions do not qualitatively change under small variation either of the value of d and/or of the diatomic bond distance.

Covalent radii and other parameters used in the calculations are standard literature values and are collected in Table I. The three-dimensional graphics have been carried out by a computer program named CACAO, described elsewhere.[40]

For each reaction we show (i) the molecular orbital interaction diagram including the atomic orbital used and (ii) the computed Walsh diagram, with the shape of selected orbitals. Where available, we compare data with previous ab initio and/or semiempirical calculations and with experimental insights. The results are discussed separately for each family of reactions. X and Y will denote a halogen atom and M a metal atom.

The X + H_2 Reaction. Consider first the very well studied F + H_2 reaction.[4,41] Both the ab initio computations[42] and the best semiempirical LEPS-type surface[43] concur that the lowest energy barrier is for a collinear configuration. The recently noted apparent disagreement of dynamical computations using this surface with experiment[44] had led to a purely empirical modification of the LEPS function which predicts a flat bent potential with a noncollinear lowest saddle point.[45] This does seem to improve the agreement with the experiment and there is a preliminary ab initio computation[46] showing that higher order correlation effects lead to the lowering of the bending potential.

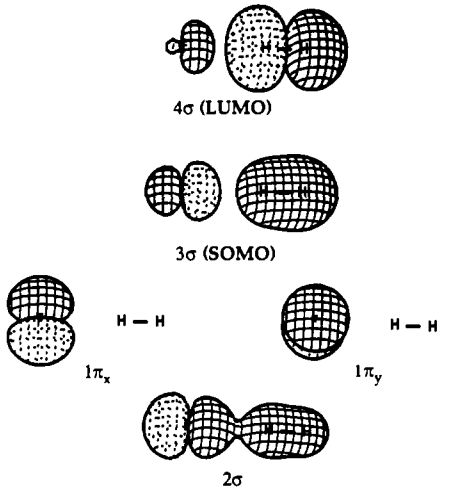

Figure 1. Selected molecular orbitals for the reaction F + H–H in the linear approach.

The orbital interaction diagram for F + H_2 is shown in **I**. The labeling of the molecular orbitals correspond to both the linear ($C_{\infty v}$) and bent (C_s) symmetry.

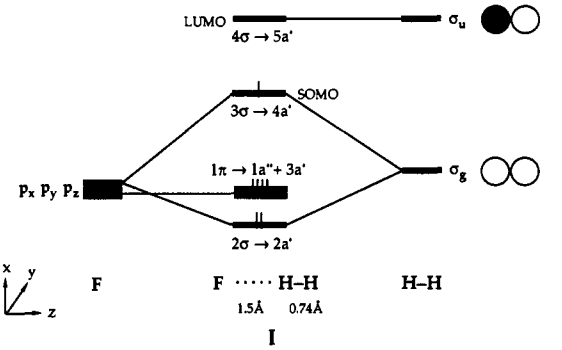

I

There are a total of nine valence electrons in this system, of which seven are shown in **I**. The 1σ orbital, almost entirely F 2s, is omitted. It should be noted explicitly here that our MO numbering system is designed for valence-electron calculations. In all electron computations the F 1s would be 1σ, and the 2s 2σ and what we call 2σ would be labeled 3σ. The highest populated molecular orbital, which may be described as an out-of-phase combination of the σ_g bonding MO of H_2 and the fluorine p_z orbital (see molecular orbital 3σ in Figure 1), is singly occupied. We call this critical orbital SOMO (singly occupied molecular orbital).

The SOMO 4a′ is an antibonding orbital, and the increase in energy due to the occupancy of this orbital is largely responsible for the (small) activation barrier for the reaction. This suggests that the dynamics of the ion–molecule $F^+ + H_2$ reaction[47] would be of interest, except for possible complexity due to nonadiabatic coupling with the F + H_2^+ channel.

We explore nonlinear approaches of F by varying the angle θ from 180 to 90°, keeping all the distances constant (**II**).

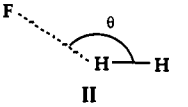

II

The calculated Walsh diagram is shown in Figure 2 (top). The dashed line on the diagram is the total energy of the system on a scale which is the same as that of the orbital energies. On the bottom we illustrate the shape of the 4a′ SOMO along the six studied steps of the distortion. The increase of antibonding re-

(39) Ammeter, J. H.; Bürgi, H.-B.; Thibeault, J. C.; Hoffmann, R. *J. Am. Chem. Soc.* **1978**, *100*, 3686.
(40) Mealli, C.; Proserpio, D. M. *J. Chem. Educ.* **1990**, *66*, 399.
(41) Steinfeld, J. I.; Francisco, J. S.; Hase, W. L. *Chemical Kinetics and Dynamics*; Harper and Row: New York, 1989.
(42) Schaefer, H. F., III *J. Phys. Chem.* **1985**, *89*, 5366.
(43) Muckermann, J. T. In *Theoretical Chemistry*; Henderson, D., Ed.; Academic Press: New York, 1981.
(44) Neumark, D. M.; Woodtke, A. M.; Robinson, G. N.; Hayden, C. C.; Lee, Y. T. *J. Chem. Phys.* **1985**, *82*, 3048.
(45) Takayanagi, T.; Sato, S. *Chem. Phys. Lett.* **1988**, *144*, 191. See also Pattengil et al. (Pattengil, M. D.; Zare, R. N.; Jaffe, R. L. *J. Phys. Chem.* **1987**, *91*, 5498) for a different possible empirical modification of the LEPS functional form.
(46) Schwenke, D. W.; Steckler, R.; Brown, F. B.; Truhlar, D. G. *J. Chem. Phys.* **1986**, *84*, 5706.
(47) Stowe, G.; Armentrout, P. B. Private communication.

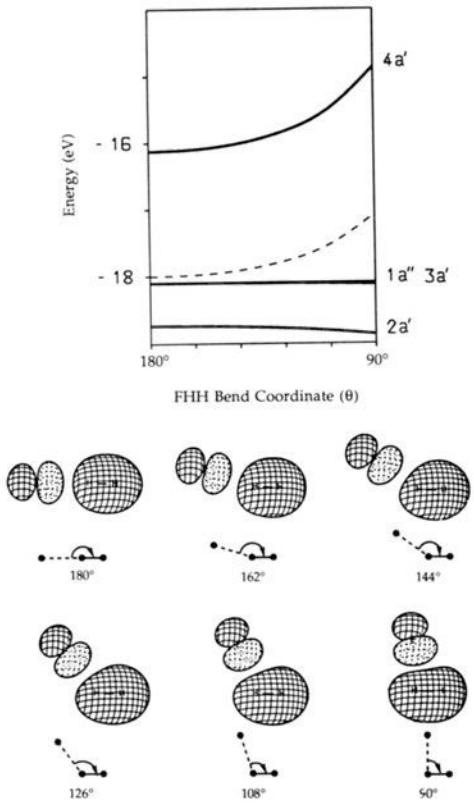

Figure 2. Walsh diagram for the reaction F + H–H (top), with the shape of the SOMO 4a′ along the distortion (bottom).

pulsion between fluorine and the two hydrogens (which is what originally destabilized this combination) explains the rise in energy of this level, and with it of the total energy. The collinear approach is then preferred.

The near-parabolic increase of the 4a′ level with bending angle vs the linear decrease of the 3a′ and 2a′ molecular orbitals suggests the in principle existence of a possible bent transition state, provided that the energy of the latter MO's decreases with the bending angle faster than we find in the computation. Our results for the other halogens (vide infra) suggest that such would be the case for an atom even more electronegative than fluorine (e.g. Ne^+).

Substitution of fluorine by other halogens does not change our qualitative results. The less electronegative atom (Cl, Br, I) shifts the *n*p orbitals to higher energy. The more diffuse p orbitals have, at the same distance, stronger overlap and consequently stronger antibonding interaction with H_2 σ_g in the SOMO. The collinear approach is always preferred and more so the heavier the halogen.

The X + HX Reaction. For the reaction F + HF, the SOMO 6a′ is a combination of two fluorine p_z orbitals, with almost no contribution from the hydrogen. There is also a greater mixing of the incoming F (see **III** and Figure 3).

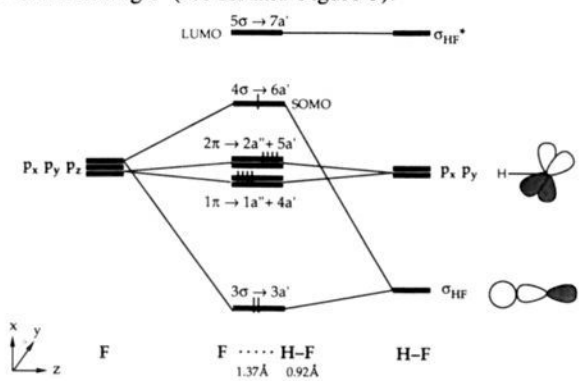

III

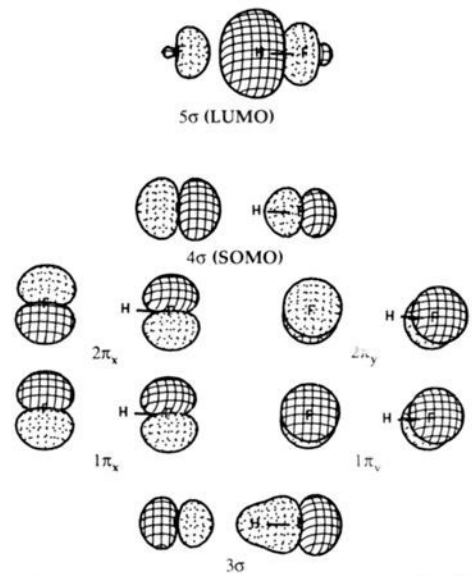

Figure 3. Selected molecular orbitals for the reaction F + H–F in the linear approach.

The orbitals here are closely related to those of a symmetric F···H···F, a system well-explored in the anion case. In the centrosymmetric molecule we would have the following level structure (**IV**). Note how the orbitals of Figure 3 are small perturbations of these.

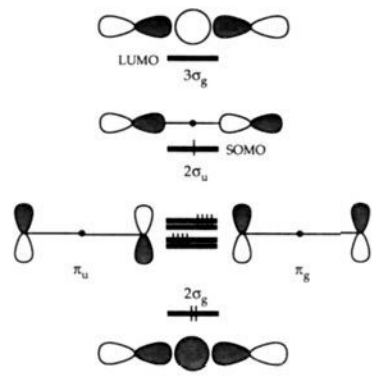

IV

The Walsh diagram for the approach of the fluorine at different θ is shown in Figure 4. The shape of the SOMO shows (Figure 4, bottom) that the lobe of the p orbital of the fluorine in HF is deformed by mixing the H 1s in a bonding way in the wave functions. The interaction with the incoming F is more antibonding. The total energy rises and therefore the collinear approach is preferred.

Substitution of fluorine by heavier halogens has the same effect as in X + H–H. The more diffuse orbitals interact strongly in the SOMO. The collinear geometry is the more stable (see for example Figure 5 for Cl + H–Cl).

We can compare our qualitative results with the calculated potential barrier reported by Last and Baer[14] for different geometries:

reaction	ΔE (eV) = $E(90°) - E(180°)$
F + HF	0.45
Cl + HCl	1.28
Br + HBr	1.37
I + HI	1.42

These results confirm that the collinear approach is always preferred and this effect increases as one moves down group 17.

For other DIM computation including the role of spin–orbit interaction see ref 48. Ab initio results for this reaction, discussed

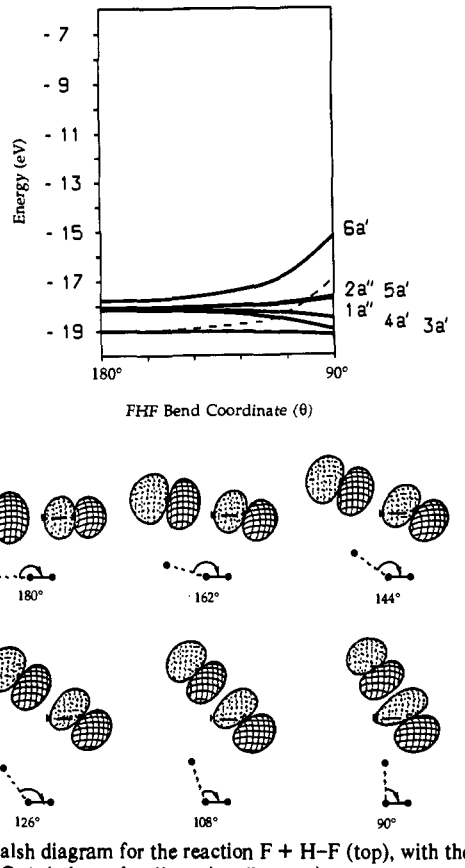

Figure 4. Walsh diagram for the reaction F + H-F (top), with the shape of the SOMO 6a′ along the distortion (bottom).

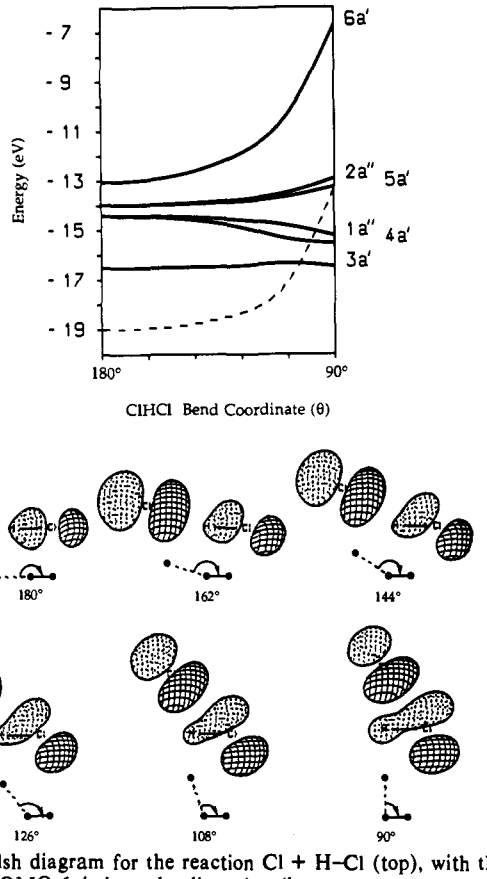

Figure 5. Walsh diagram for the reaction Cl + H-Cl (top), with the shape of the SOMO 6a′ along the distortion (bottom).

in ref 49, show a slightly bent (by about 1 kcal·mol^{-1}) lowest saddle point. An overview is given in ref 6.

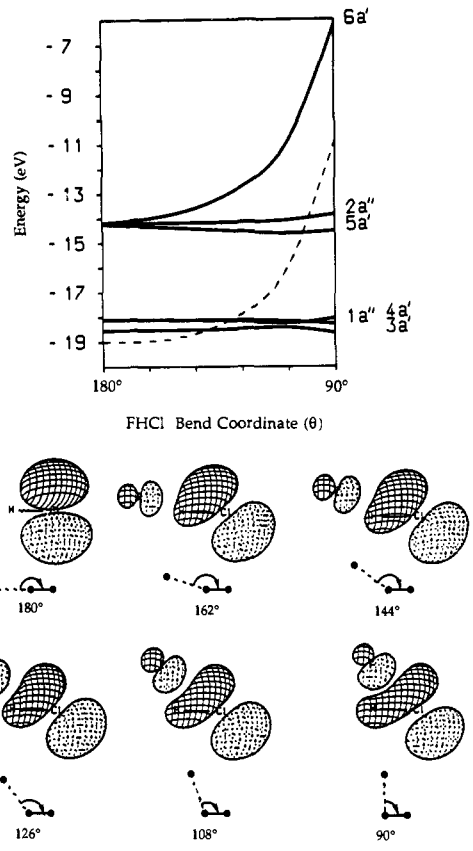

Figure 6. Walsh diagram for the reaction F + H-Cl (top), with the shape of the SOMO 6a′ along the distortion (bottom).

The X + HY Reaction. Consider the general exchange reaction X + HY, where X is the most electronegative atom. The resulting interaction diagram is shown in **V**. The doubly degenerate HOMO (highest occupied molecular orbital) is formed by the nonbonding p orbitals centered on Y. For a total electron count of 15 the HOMO is triply occupied.[50]

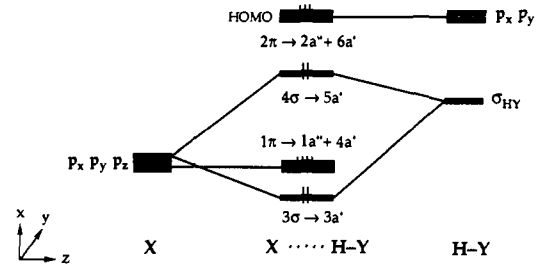

V

As an example we take F + HCl (see Figure 6). The distortion ($C_{\infty v} \rightarrow C_s$) removes any degeneracies. The SOMO changes from nonbonding (p_x on Cl) to antibonding, raising the total energy for the bent approach. We found the same results substituting the two halogens in different combinations (F + HBr, F + HI, Cl + HBr, Cl + HI, etc.). Note that this implies that the dynamics of the anionic ion–molecule reactions, e.g. F^- + HBr, will be governed by a potential energy function qualitatively similar to that for the neutral reaction, as is indeed observed.[51]

(48) Duggan, J. J.; Grice, R. *J. Chem. Soc., Faraday Trans. 2* **1983**, *80*, 739. Firth, N. C.; Grice, R. *Ibid.* **1987**, *83*, 1023.

(49) Garrett, B. C.; Truhlar, D. G.; Wagner, A. F.; Dunning, T. H. *J. Chem. Phys.* **1983**, *78*, 4400.

(50) In principle there are two configurations possible for the X···H-Y system: $(4\sigma)^2(2\pi)^3$ and $(4\sigma)^1(2\pi)^4$. The former is what one might expect from the attack of a ground-state X atom on H-Y, and the latter is likely to be the ground state of the composite system. The analysis presented here is for the $(4\sigma)^2(2\pi)^3$ configuration; if the other one is assumed, the preference for the collinear approach is only emphasized due to double occupation of the controlling 6a′ level.

Consider now X less electronegative than Y. In interaction diagram **VI**, the SOMO is a combination of p_z orbitals, now centered on the approaching atom.

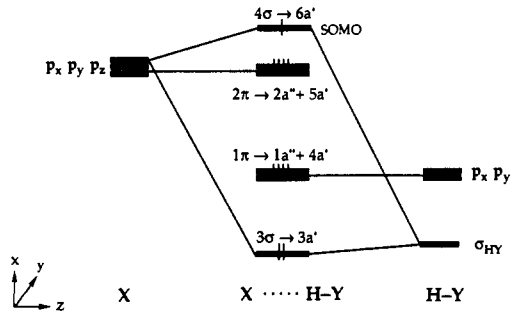

VI

Decreasing the angle θ raises the SOMO, as a consequence of increased antibonding interaction between the p orbitals (see Figure 7 for Cl + HF). We found the same results for different halogens (Br + HF, I + HF, I + HCl, etc.). In both possible cases the collinear approach is preferred.

The H + X_2 Reaction. We consider first H + Cl_2 and the interaction diagram in **VII**. The SOMO is an antibonding combination between the s orbital of the incoming hydrogen and the σ_g orbital of Cl_2.

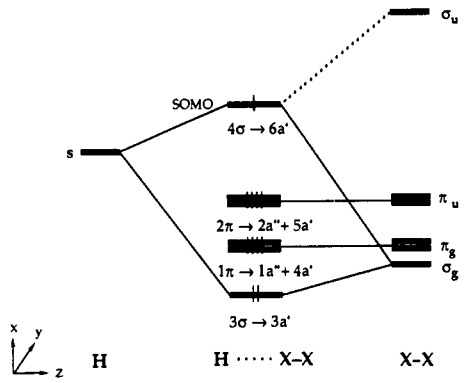

VII

In this case the bent approach is slightly favored, as shown by the total energy curve (dashed line) in the Walsh diagram in Figure 8. We notice that the energy stabilization for this class of reactions is always small compared to the barrier encountered in the previous reactions.

The stabilization of the system is governed by a bonding interaction between the H and one component of the π_u level of X_2 (level 5a' in Figure 8, bottom). The energy of the SOMO passes through a maximum because the interaction of the H is shared between the σ_g and σ_u orbitals of the diatomic X_2. Interaction with σ_g destabilizes the H 1s orbital, while mixing with σ_u stabilizes it. This is a new feature in these diagrams, and one expected whenever one molecular component has relatively low-lying unoccupied MO's. The two levels 7a' (LUMO) and 6a' (SOMO) generate the pattern characteristic of symmetry-avoided crossing.

The reaction for heavier halogens prefers the bent approach, as suggested by the experiments.[52] The more diffuse π orbitals interact strongly with hydrogen coming from the side.

For H + F_2 the influence of the SOMO on the total energy is stronger (see Figure 9), with the result of a small barrier around 145°. The approach from the side appears to be energetically preferable. This is in disagreement with ab initio calculations on H + F_2.[53,54] Further, unpublished calculations show that the

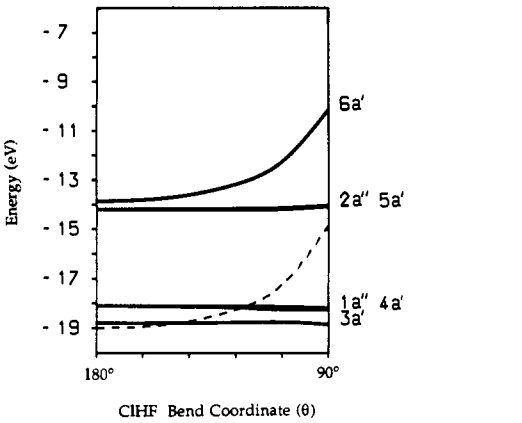

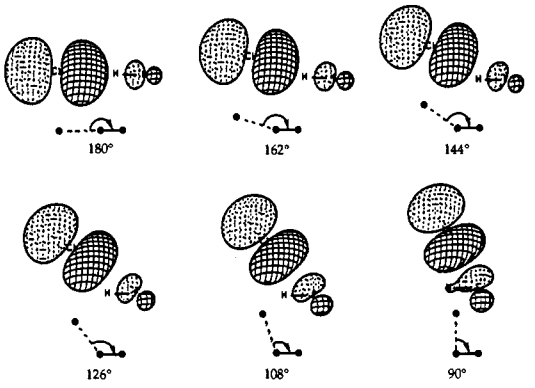

Figure 7. Walsh diagram for the reaction Cl + H–F (top), with the shape of the SOMO 6a' along the distortion (bottom).

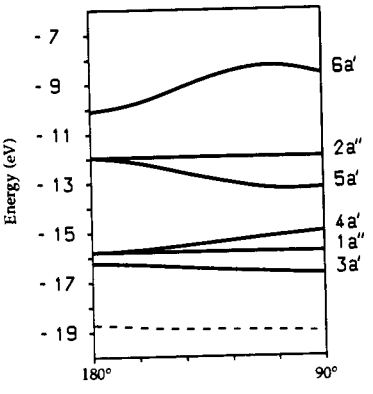

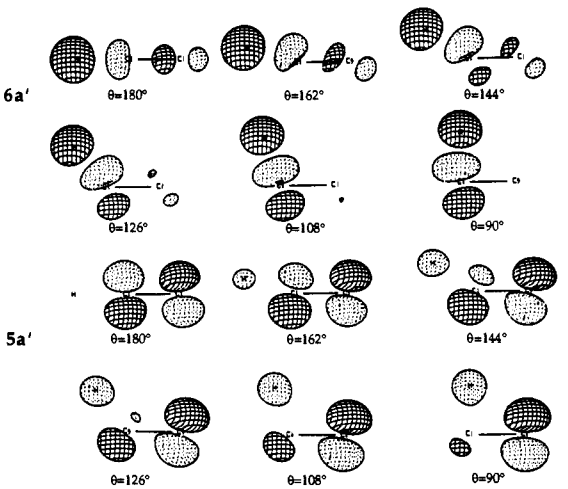

Figure 8. Walsh diagram for the reaction H + Cl–Cl (top), with the shape of the SOMO 6a' (center) and the level 5a' (bottom) along the distortion.

(51) Langford, A. O.; Bierbaum, V. M.; Leone, S. *J. Chem. Phys.* **1985**, *83*, 3913.
(52) Smith, I. W. M. *Kinetics and Dynamics of Elementary Gas Reactions*; Butterworths: London, 1980.
(53) Bender, C. F.; Bauschlicher, C. W., Jr.; Schaefer, H. F., III *J. Chem. Phys.* **1974**, *60*, 3707.
(54) Eades, R. A.; Dunning, T. H., Jr.; Dixon, D. A. *J. Chem. Phys.* **1981**, *75*, 2008.

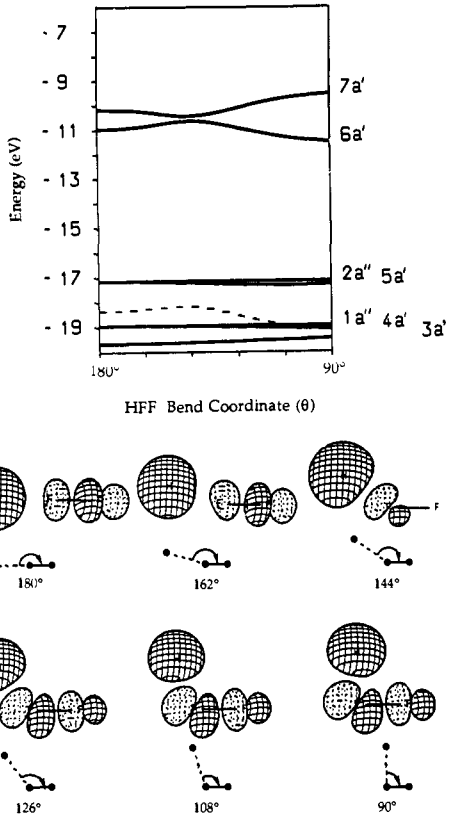

Figure 9. Walsh diagram for the reaction H + F-F (top), with the shape of the SOMO 6a′ along the distortion (bottom).

energy rises monotonically from 180 to 90°.[55]

The H + Cl_2 reaction has received considerable attention using both LEPS-type[56,57] and empirical potentials adjusted so as to agree with the experimental results,[58,59] as well as ab initio calculations.[60] It is for this well-studied example that the predictive power of molecular orbital theory is quite clear. The LEPS-type and the empirical potential functions favor a collinear approach, unlike the bent approach discussed above. Ab initio calculations predict that the saddle point is bent by ~20°.[60]

For the H + Br_2 reaction ab initio calculations favor a collinear approach,[61] although dynamical simulation[62] indicates that the factors controlling the angular distribution are more complicated.

The H + XY Reaction. To account for the interaction of H with XY we have to understand the composition of various XY orbitals. **VIII**, left, shows the σ orbitals of a homonuclear diatomic Z_2 (e.g. Br_2). $1\sigma_g$ is the Z-Z σ bond,[63] $1\sigma_u$ and $2\sigma_g$ the antisymmetric and symmetric lone pair combinations, and $2\sigma_u$ the Z-Z σ^* level.

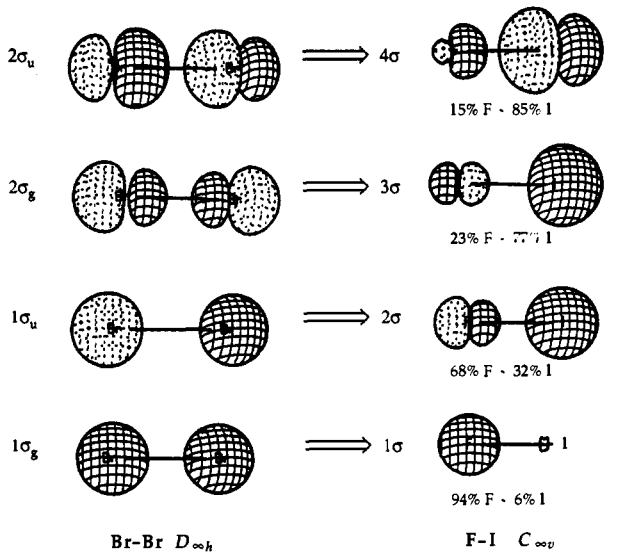

VIII

Now suppose an "electronegativity perturbation" takes place, i.e. $Z_2 \rightarrow XY$, where X is more electronegative than Z and Y less electronegative. Simple perturbation theory[64] shows that in such a case formerly symmetric orbitals localize in such a way that the lower member of a paired set (bond or lone pair) localizes on the more electronegative atom, while the upper member localizes on the less electronegative. If X is more electronegative than Y (see e.g. for FI, **VIII** right), this means that $1\sigma_g$ ($\rightarrow 1\sigma$ in $C_{\infty v}$) and $1\sigma_u$ ($\rightarrow 2\sigma$) are localized on X, while $2\sigma_g$ ($\rightarrow 3\sigma$) and $2\sigma_u$ ($\rightarrow 4\sigma$) localize on Y. With respect to interaction with incoming H, as we have seen for H + X_2, 3σ is most important. *This orbital is localized on the less electronegative atom*, as shown in **VIII** for FI. This effect is evident in the energy of the SOMO shown in **IX** for the possible reactions H + FI and H + IF.[65] The SOMO for H + IF is more stable by 5.4 eV.

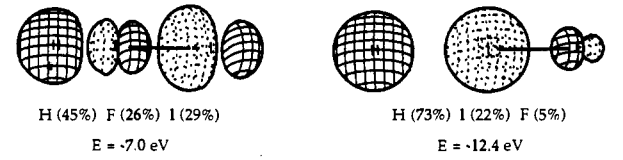

IX

The analysis of the Walsh diagram for the bent reaction presents features similar to those for H + X_2, with the bent approach slightly preferred. An ab initio comparison of the trends in these two families is available.[54] Interestingly, both ab initio[54] and semiempirical calculations (details not given here) indicate a preference for the linear approach for the less favored attack of H on the more electronegative atom.

The M + X_2 and M + XY Reactions. In this class of reactions M is an alkali metal. It is known that for these reactions a so-called "harpoon" mechanism[4,66] obtains, i.e. at large separations (>5 Å) one electron is transferred from the metal to the molecule. This jump is governed by the small difference between the ionization potential of the metal and the electron affinity of the molecule. At short range, where orbital interaction effects are important, the governing surface can be thought of as that of $M^+ + X_2^-$. The orbitals of the metal should now be less diffuse. We simulated this by increasing the exponent of the Slater function to a mean value of 1.1.[67] To effect the electron transfer we

(55) Eades, R. A. Ph.D. Thesis, University of Minnesota, 1983. We are grateful to the reviewer for bringing 53-55 to our attention.
(56) Ding, A. M. G.; Kirsch, L. J.; Perry, D. S.; Polanyi, J. C.; Schreiber, J. L. *Faraday Discuss. Chem. Soc.* **1973**, *55*, 252. Parr, C. A.; Polanyi, J. C.; Wong, W. H.; Tardy, D. C. *Faraday Discuss. Chem. Soc.* **1973**, *55*, 308.
(57) Baer, M. *J. Chem. Phys.* **1974**, *60*, 1057; **1975**, *62*, 4545. Wilkins, R. L. *J. Chem. Phys.* **1975**, *63*, 2963. Polanyi, J. C.; Schreiber, J. L.; Sloan, J. *J. Chem. Phys.* **1975**, *9*, 4033. Pattengill, M. D.; Polanyi, J. C.; Schreiber, J. L. *J. Chem. Soc., Faraday Trans. 2* **1976**, *72*, 897. Fischer, S.; Venzl, G.; Robin, J.; Ratner, M. A. *Chem. Phys.* **1978**, *27*, 251. Venzl, G.; Fischer, S. F. *Chem. Phys.* **1978**, *33*, 305.
(58) Connor, J. N. L.; Jakubetz, W.; Manz, J.; Whitehead, J. C. *J. Chem. Phys.* **1983**, *72*, 6209.
(59) Connor, J. N. L.; Jakubetz, W.; Laganà, A.; Manz, J.; Whitehead, J. C. *Chem. Phys.* **1982**, *65*, 29.
(60) Private communication from a reviewer.
(61) Baybutt, P.; Bobrowicz, F. W.; Kahn, L. R.; Truhlar, D. G. *J. Chem. Phys.* **1978**, *68*, 4809.
(62) Blais, N. C.; Truhlar, D. G. *J. Chem. Phys.* **1974**, *61*, 4186.
(63) Both $1\sigma_g$ and $2\sigma_g$ contribute to Br-Br σ bonding. But more of that bonding is to be allocated to $1\sigma_g$, which contributes 60% of the total Br-Br σ overlap population.
(64) Jorgensen, W. L.; Salem, L. *The Organic Chemist's Book of Orbitals*; Academic Press: New York, 1974.
(65) Our calculations thus give substantial electron density on the central atom. This disagrees with conclusions based on calculations by D. A. Dixon for the A + BC system, cited in: Truhlar, D. G.; Dixon, D. A. *Atomic-Molecule Collision Theory*; Bernstein, R. B., Ed.; Plenum: New York, 1979; Chapter 18.
(66) Davidovits, P.; McFadden, D., Eds. *The Alkali Halide Vapors*; Academic Press: New York, 1979.

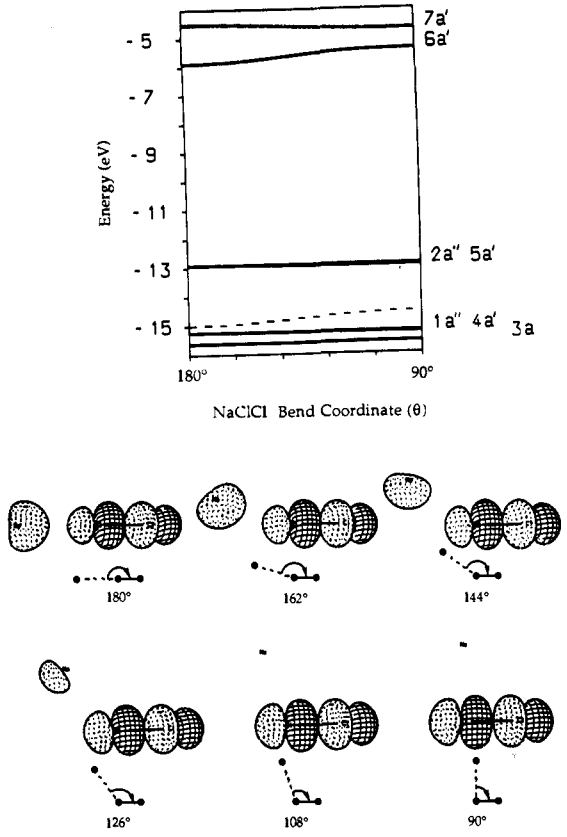

Figure 10. Walsh diagram for the reaction Na + Cl–Cl (top), with the shape of the SOMO 6a′ along the distortion (bottom).

elongated the X_2 distance, lowering the energy of the X_2 σ_u. This is the acceptor orbital for the electron transferred from M. For our computation we choose the approach distance so that for the collinear reaction the charge on the metal is near +0.8 and the OP (M···X_2) near 0.1.

The interaction diagram **X** shows that the SOMO is the bonding combination of the σ_u from X_2 and the s orbital from M.

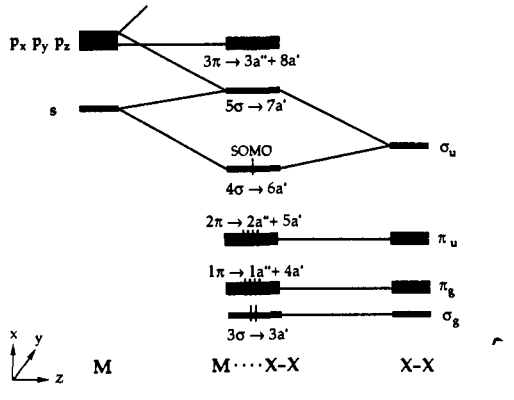

X

Now we consider as an example the Na + Cl_2 reaction, with the Walsh diagram in Figure 10. The energy of the SOMO 6a′ increases along the distortion. The contribution of the metal s AO in the molecular orbital decreases. The collinear approach is slightly preferred, for all possible reactions, by 0.2–0.4 eV. This is in accord with DIM computations[68] and with indications provided by ab initio computations.[69,70]

For the reaction M + XY, there is no preference for attack on one or the other of the two halogens, the interaction with the σ_u of the elongated molecule being approximately equal for both sides. We find that the linear approach is slightly preferred in either case.

We reach the same conclusion when M is substituted by metals of group 2. The 6a′ level is now doubly occupied, and the linear approach is preferred.

The M + XH Reaction. For the hydrogen halides the long-range harpoon mechanism is no longer valid. The transfer of one electron could occur only at small separation where the orbital interaction effects are important. For this reaction we adopt the usual approach, keeping the HX distance at the equilibrium value. The diagram is similar to **X**, but the interaction between the metal s AO and the empty antibonding σ^* orbital of XH is now weaker. The frontier orbitals do not change for all the possible reactions (e.g. Li + FH, Na + IH), and the Walsh diagrams do not vary much. The total energy increases slightly from 180 to 90°, but by less than 0.1 eV. It seems a wide range of approach angles is available for this class of reactions.

We can improve the charge transfer from the metal to the molecule, as we did before, by elongating the H–X bond so as to lower the σ_u level. The result is a preferred linear geometry as for M + X_2. Our results are more in accord with DIM computations[71] than with the bent configuration predicted by ab initio methods[72-74] for both Li + HF and Li + HCl, with the stretched H–X bond at the transition state. As a reviewer has pointed out, the saddle points for the M + XH reaction are in the exit channel, a stable M···X–H intermediate being formed. It may be that in this case our calculations, which probe the beginnings of the exchange reaction, i.e. the entrance channel, are not relevant.

The X + X_2, Y + X_2, and X + XY Reactions. The interaction diagram for X + X_2 is shown in **XI**. The system has a total of 21 electrons, with the SOMO an antibonding combination between the incoming X(p_z) and the σ_g of X_2.

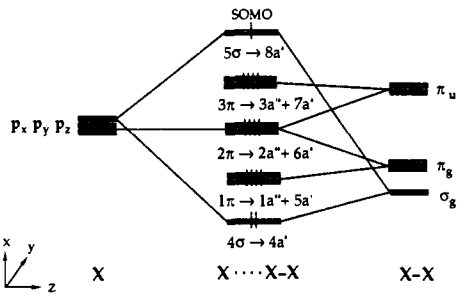

XI

In the Walsh diagram for the Br + Br_2 reaction (see Figure 11), the levels 8a′ (SOMO) and 7a′ are strongly affected by the distortion.

The preferred geometry depends on the energy balance between the doubly occupied 6a′ and the singly occupied 7a′. Our results shown that the total energy curve is flat for F + F_2 and Cl + Cl_2, with a shallow minimum at 145° (ca. 0.15 eV) for Br + Br_2, decreasing linearly to 90° (ca. 0.37 eV) for I + I_2. The DIM results[75] show the bending already for Cl + Cl_2. A system with 22 electrons (X^- + X_2) will prefer the linear approach.

We also consider the reaction between different halogens, Y + X_2. The relative position of the FMO's interacting in **XI** is different, but the nature of the SOMO, the antibonding combination between p_z and σ_g, is always 8a′ in all possible reactions from F + I_2 to I + F_2. The bent approach (ca. 145°) is most stable, with a relative minimum of 0.2–0.4 eV.

(67) For a STO the exponent ζ is proportional to Z^*/n. Increasing the charge by one we obtain $\zeta' = (\zeta + 1/n)$. The mean value for the alkali metals is 1.1.
(68) Zeiri, Y.; Shapiro, M. *J. Chem. Phys.* **1981**, *75*, 1170.
(69) Balint-Kurti, G. G. *Mol. Phys.* **1973**, *25*, 393.
(70) Maessen, B.; Cade, P. E. *J. Chem. Phys.* **1984**, *80*, 2618.
(71) Shapiro, M.; Zeiri, Y. *J. Chem. Phys.* **1979**, *70*, 5264.
(72) Chen, M. M. L.; Schaefer, H. F., III *J. Chem. Phys.* **1980**, *72*, 4376.
(73) Garcia, E.; Laganá, A.; Palmieri, A. *Chem. Phys. Lett.* **1986**, *127*, 73.
(74) Palmieri, A.; Garcia, E.; Laganá, A. *J. Chem. Phys.* **1988**, *88*, 181.
(75) Duggan, J. J.; Grice, R. *J. Chem. Soc., Faraday Trans. 2* **1984**, *80*, 795, 809.

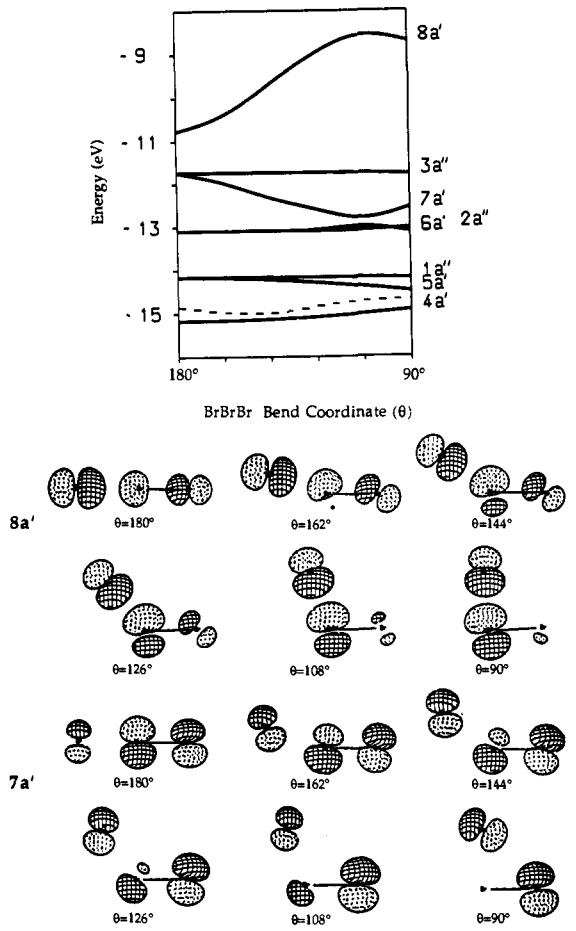

Figure 11. Walsh diagram for the reaction Br + Br–Br (top), with the shape of the SOMO 8a′ (center) and the level 7a′ (bottom) along the distortion.

The most general set of reactions Z + XY, with three different halogens, and X + XY does not present new features. As for H + XY, the attack on the less electronegative atom is energetically favored. The Walsh diagram for the bent reaction is very similar to the one in Figure 11, the approach on the side being slightly stabilized in all cases examined. The position of the minimum changes from 145 to 90° for different combinations of halogens, but the stabilization is never more than 0.6 eV. These trends are consistent with the early experimental results.[76]

The O(^{3}P) + XH and O(^{3}P) + XY Reactions. In all reactions examined the intermediate complex (radical) usually corresponds to a molecular species which correlates with the ground state of reactants and products. In the reaction with oxygen, however, different spin states are involved. To analyze the O(^{3}P) + HX reaction we can use the interaction diagram in **VI**. Because oxygen is in a ^{3}P state we remove one electron from the inner level, doubly degenerate, under the SOMO. The final state with 14 electrons is now a triplet that correlates with the reactants. The resulting Walsh diagram for the distorted approach is similar to that in Figure 7 and so is the total energy. The triplet state prefers the linear approach, and the rapid barrier rise for angles below 145° or so is as assumed in the empirically optimized LEPS surface.[77] The most recent ab initio results[78] suggest however a shallow off-collinear minimum.

In the same way we can examine O(^{3}P) + XY looking at **XI** and Figure 11. We are making the assumption, supported by actual calculations, that the qualitative features of the X + XX diagram carry over to Z + XY. For the same overlap reason as before, the attack on less electronegative halogen is preferred. The electron is removed from one of the inner levels that transforms as 6a′ and 2a″ in C_s symmetry. These levels are unaffected by the bending, and as a consequence the total energy depends again on the balance between the SOMO 8a′ and the 7a′. We found that the bent (ca. 145°) approach is stabilized.

Concluding Remarks and Prospects

The results reported show that orbital considerations and their quantitative expression as Walsh diagrams can be used to determine the atomic orientation near the barrier for exchange reactions. Even if not quantitatively accurate, the extended Hückel approach captures the chemical systematics when s and p orbitals are important. Since there are clear reactivity trends with d orbital occupancy,[79,80] it would be desirable to apply such considerations to them as well.

Another important direction is to determine the entire potential energy function. In particular, there is a clear need to extend the LEPS functional form with its collinearly preferred approach to an analytical form valid also when p orbitals are involved. Molecular orbital considerations clearly establish why a collinear approach is expected for s orbitals. The present results show that the method can discern between collinear and sideways approach when p orbitals are occupied. It can even account for variations within a given family (as in X + X_2, from collinear for F + F_2 to completely bent for I + I_2). It remains, however, to provide an analytical representation of such systematics.

Acknowledgment. This work began when one of us (R.D.L.) visited Cornell University. He would like to thank the A. D. White Professor-at-Large program for the opportunity to come to Cornell and the members of the Baker Laboratory for their warm hospitality. We thank the Consiglio Nazionale delle Ricerche (CNR-Italy) for the award of postdoctoral fellowships for D.M.P. and the National Science Foundation for its support through Grant CHE-8912070. A knowledgeable reviewer and D. G. Truhlar made some very useful comments on our work.

(76) Lee, Y. T.; LeBreton, P. R.; McDonald, J. D.; Herschbach, D. R. *J. Chem. Phys.* **1969**, *51*, 455.
(77) Persky, A.; Broida, M. *J. Chem. Phys.* **1984**, *81*, 4352.
(78) Gordon, M. S.; Baldridge, K. K.; Bernhold, D. E.; Bartlett, R. J. *Chem. Phys. Lett.* **1989**, *158*, 189.
(79) Hoffmann, R. *Science* **1981**, *211*, 995 and reference therein.
(80) Elkind, J. L.; Armentrout, P. B. *J. Phys. Chem.* **1987**, *91*, 2037.